ISSN (O): 2393-8609

International Journal of Aerospace and Mechanical Engineering

Volume 4 – No.2, April 2017

DESIGN, ANALYSIS AND FABRICATION OF MICRO CLASS UAV

Ram Rohit Vannarth
Assistant Professor
Dept. of Mechanical Engineering
B M S College of Engineering, Bangalore
ramrohit.mech@bmsce.ac.in

Srinath Kulkarni
Student, B.E
Dept. of Mechanical Engineering
B M S College of Engineering, Bangalore
srinathmaheshkulkarni@gmail.com

Dr. Kayala Mallikharjuna Babu
Principal
Dept. of Mechanical Engineering
B M S College of Engineering, Bangalore
principal@bmsce.ac.in

ABSTRACT

Design of an aircraft is a complicated process and requires a lot of analysis to reach conclusions. This paper discusses about the design of the aircraft and the analysis that is required to make the UAV. The UAV discussed in this paper can carry a payload fraction of 0.7 and has a self-weight of 350g. XFLR5 software is used to analyse the airfoil in 2D. The analytical approach is discussed in detail for the design of the Unmanned ariel vehicle(UAV).

Keywords

Unmanned ariel vehicle(UAV), Drag analysis, Airfoil, Balsa Wood, Fuselage, Tail, Wing

1. INTRODUCTION

1.1 History

Unmanned Aerial Vehicles (UAVs) have been around for centuries and were solely used for military purposes. The earliest recorded use of a UAV dates back to 1849 when the Austrians attacked the Italian city of Venice using unmanned balloons that were loaded with explosives. Although balloons would not be considered a UAV today, this was a technology the Austrians had been developing for months before, which led to further advancements. In 1915, British military used aerial photography to their advantage in the Battle of Neuve Chapelle. They were able to capture more than 1,500 sky view maps of the German trench fortifications in the region. The United States began developing UAV technology during the First World War in 1916 and created the first pilotless aircraft. Shortly after, the U.S Army built the Kettering Bug. While continuing to develop UAV technology, in 1930 the U.S Navy began experimenting with radio-controlled aircraft resulting in the creation of the Curtiss N2C-2 drone in 1937. During WWII, Reginald Denny created the first remote-controlled aircraft called the Radioplane OQ-2. This was the first massed produced UAV product in the U.S and was a breakthrough in manufacturing and supply drones for the military.

Drones were previously known to be an unreliable and an expensive toy, but in the 1980's this attitude began to change. The Israeli Air Force's victory over the Syrian Air Force in 1982 contributed to this change. Israel used both UAVs and manned aircraft to destroy dozen of Syrian aircraft with minimal losses. Further in the 1980's, The U.S created the Pioneer UAV Program to fulfill the need for inexpensive and unmanned aircraft for fleet operations. In 1986 a new drone was created from a joint project between the U.S and Israel. The drone was known as RQ2 Pioneer, which was a medium sized reconnaissance aircraft.

Although many of the most notable drone flights have been for military purposes, technology is continuing to advance and receive more attention. In 2014, Amazon proposed using UAVs to deliver packages to customers and some real-estate companies are using drones to shoot promotional videos. The uses of drones will continue to grow in many industries worldwide.

1.2 Approach

Typical approach to this is usually to design a plane equipped with its own propulsion system, adopt the more innovative concept of plane. The empty weight was reduced to a minimum extent possible. This opened a whole new level of possibilities on constructing wing with less weight and with higher structural strength.

This plane can successfully fly in air with precision using radio controls. The motor used is a high thrust, less weight motor which will satisfy our thrust requirements of the plane. The fuselage is derived from the conventional design and modified to the constraints of our needs. This plane was designed to achieve a payload fraction of 0.7, hence making some ground breaking research in making the plane more light considering structural strength. The plane weighed less than 350g. Considering all constraints payload fraction achieved was 0.7.

2. DESIGN PROCEDURE

2.1 Figure of Merit (FOM)

Table 1. FOM Table for different configurations

Plane Name	Conventional	Biplane	Flying Wing
Lift Capacity	3.5	4.0	3.5
Stability	4.0	4.0	3.5
Ease of Construction	4.0	2.5	2.5
Historical Data	4.0	3.5	3.0
Cost	4.0	3.0	3.0
TOTAL	19.5	17.0	15.5

Configuration selection is one of the main considerations for building the plane. Three basic configurations of the plane are considered namely: Conventional, Biplane and Flying wing. The comparison shows quantitatively how different configurations perform across a range of design requirements. Figure of merit (FOM) is used to decide, with the maximum of 5 points allotted to each parameter. The conventional wing

ISSN (O): 2393-8609

International Journal of Aerospace and Mechanical Engineering

Volume 4 – No.2, April 2017

configuration showed superiority over the other configurations. Payload bay accessibility in the biplane was constricted by the lower wing and the fabrication was also time consuming and complex. In flying wing configuration, room for payload bay is less and the configuration would not allow us much space to fit all the components in the plane.

The conclusions obtained from this analysis is that the conventional configuration of plane is best requirement for requirements because of high 'CL' value at given Reynolds number, the ease of construction, historical data available, structural simplicity and its cost involved.

2.2 Airfoil Selection

A study was conducted on a wide range of airfoils. Among many airfoils suitable for high lift application E423, MH45, S1210 and NACA4412 airfoils were analyzed using XFLR5 software. Using an estimated Reynolds number of 100000, the analyzed sectional lift co-efficient for different airfoils is shown in fig1. The airfoil coordinates are obtained from the UIUC Airfoil Coordinates Database. The lift curves and moment polars are compared. The drag polar shows the superiority and lower pitching moment of the E423 airfoil which shows superiority over other airfoils. Finally E423 airfoil is selected which has high lifting capabilities at low Reynolds number. To increase the efficiency of the wing and to obtain highest CL value, angle of attack of 60 where the foil will have CL value greater than one and also highest L/D ratio. The small amount of waviness in the graphs is due to numerical instabilities and convergence errors at low Reynolds numbers.

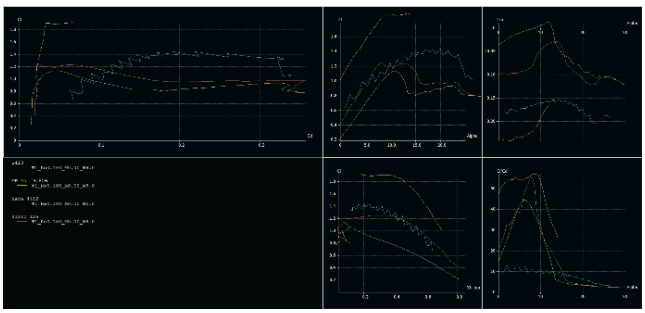

Fig 1: Analysis of Different foil in XFLR5 software

2.3 Planform Selection

Design of the wing depends on the wing size, lift capacity, wing loading, ease of construction and drag effects. The ideal planform of the wing for minimum drag is elliptical, but due to its complexity in design and fabrication we chose rectangular planform which is cost effective as well as easy for fabrication. To reduce the wing tip vortices which is one of the adverse effects of the rectangular planform was done by designing the winglets which are proven performance enhancer. For an empty weight of350gand a payload fraction of 0.7, the required lift produced by the wing should be 1162g. Flight velocity of 36 ft/s was assumed based on historical data. Using XFLR-5 software initial 2D-lift coefficient is 1.2. Using the formula for the lift, the wing area required for the corresponding lift is0.148 m2.L = $\frac{1}{2}\rho v^2 AC_L$……..(1)

L - Lift gained by the wing in newtons

ρ- Density of air at the altitude in which the plane is flying

v – velocity of the free stream of air

A - area of the planform of the wing

CL – 3D lift Co-efficient of the wing

2.4 3D Lift Co-efficient

The 2-D coefficients are for wings with an infinite aspect ratio. Wings of finite aspect ratio i.e., 3 -D wings need a correction to the lift coefficient. The lift coefficient of finite wing is lower than the infinite aspect ratio wing, due to lift induced drag which manifests as wing-tip vortices reducing the overall lift coefficient. The finite wing lift curve has the same zero lift angle of attack, and pivots about this point, clockwise. The reduced slope □□l/□∝ derived from theory is given by,

$$\frac{dC_l}{d\alpha} = \frac{2\pi*(AR)}{2+\left[4+(AR\times\beta)^2\left(1+\frac{tan^2(\Lambda)}{\beta^2}\right)\right]^{1/2}} \ldots\ldots\ldots\ldots\ldots(2)$$

$$\beta = (1 - M_{eff}^2)^{1/2} \ldots\ldots\ldots\ldots\ldots\ldots(3)$$

$$M_{eff} = M_\infty \cos(\Lambda) \ldots\ldots\ldots\ldots\ldots\ldots(4)$$

AR– Aspect ratio of the wing

M_∞- Free stream mach number

M_{eff}- Effective Mach number

Λ – Sweep angle of the wing

From the above equations, $dC_l/d\alpha$ equals 0.08. Coefficient of lift for finite aspect ratio is given by the equation $C_L = dC_l/d\alpha + C_{L\alpha} = 0$

And $C_{L\alpha}$ at 0^o = 1.04. This gives a corrected C_L value of 1.48 at ∝=6°

3. ANALYSIS

3.1 Thrust analysis

The primary equation considered motor, the Thrust for a RC plane is provided by the combined effect of rotation of the motor and propeller which it is driving. The RPM of the motor and the propeller sizing defines the thrust provided by the former. So, it is inherent that motor choice and propeller sizing should be in par with each other to obtain required thrust.The primary equation considered motor selection was the relationship between the motor thrust and the RPM given below:

$$RPM = K_V \times V_{battery} \ldots\ldots\ldots\ldots\ldots\ldots\ldots(5)$$

$V_{battery}$ - Voltage delivered by the battery,
K_V - RPM per Volt.

K_V is the measure of the torque output of the brushless motor.

Lower K meant lower RPM with more thrust which was typical of slow flying planes. The trade-off study on different motors helped in selecting a motor with 1250 KV. The Propeller sizing is obtained based on the standard equation of Pitch velocity given below:

ISSN (O): 2393-8609

International Journal of Aerospace and Mechanical Engineering

Volume 4 – No.2, April 2017

$$V_{pitch} = RPM \times pitch \times \eta_{propeller} \text{ .....(6)}$$

$\eta_{propeller}$ - Efficiency of propeller

The equation used to calculate the static thrust is:

$$T = \frac{P}{V_{pitch}} \text{.....(7)}$$

P – power of motor

The static thrust was obtained to be 0.09 N.

The dependency of the Dynamic thrust on the propeller sizing and the static thrust was obtained using the equation below:

$$T_D = T \times \rho \times V^2 \times d^2$$

ρ – density of air

v – Free stream velocity

d – diameter of the propeller

A satisfactory thrust rating of 1500gis obtained using the above equation for the propeller sizing of 9 inches radius and pitch of 5 inches. So, the optimum propeller sizing is decided to be 9 X 5.

3.2 Servo Sizing:

The flight control surfaces such as Ailerons, Rudder and Elevators are controlled are operated using electrical micro servos of suitable torque and capacities. Each of the control surfaces experience a different amount of force under various conditions and thus were carefully examined for their maximum rotations in angle under normal and extreme conditions of flight. Considering the influence of external factors on the control surfaces and the overall flight, it was necessary to determine appropriate servo size. Considering the maximum velocity experienced by the flight to be around 10-12 ms^{-1}, the force exerted on the control surfaces were calculated as torques on each of the servos under maximum load and turning conditions.

The formula used to determine the required servo size is :

$$torque(oz-in) = 8.5 \times 10^{-6} \times \frac{c^2 \times v^2 \times L \times \sin(s1)}{\tan(s2)} \text{.....(8)}$$

where:

c = control surface chord in cm, L= control surface length in cm, *v* = speed in MPH, *S*1= max. control surface deflection in degrees, S2= maximum servo deflection in degrees.
Equation generates torque values for the control surfaces are as follows:

Table 2. Torque of the servos of the Control Surfaces

Ailerons-10.7 oz-in	Elevator- 92.29 oz-in	Rudder- 44.27 oz-in

3.3 Drag Analysis

The 3-D drag polar of the aircraft is approximated using equation

$$C_D = C_{Dmin} + K'C_L^2 + K''(C_L - C_{Lmin})^2 \text{.....(9)}$$

The C_{Dmin} is made up of the pressure and skin friction drag from the fuselage, wing, tails etc. K' is the inviscid or induced drag factor, C_L is the coefficient of lift at a given angle of attack, K'' is the viscous induced drag factor, and C_{Lmin} minimum coefficient of lift. The wetted area of the wing is approximated as

$$S_{wetted} = S_{exposed}\left[1.977 + 0.52\left(\frac{t}{c}\right)\right] \text{.....(10)}$$

$$if\ \frac{t}{c} > 0.05$$

C_{Dmin} is found by adding the contributions of each component as calculated in in previous equation

$$C_{Dmin} = \frac{FF \times C_f \times S_{wetted}}{S_{planform}} \text{.....(11)}$$

In above equation, FF is the form factor, C_f is the skin friction coefficient, S_{wetted} is the wetted surface area, and $S_{planform}$ describes the planform area of the components.

Table 3. Drag analysis values of different parts of plane

	WING	FUSELAGE	VERTIC-AL TAIL	HORIZONT-AL TAIL
S_{ref}(inch^2)	229.81	56.16	14.88	27.28
S_{wet}(inch^2)	469.79	182.18	30.35	55.63
S_{wet}/S_{ref}	2.044	3.244	2.0396	2.039
FF	1.229	1.076	1.222	1.222
R_{cutoff}	101659.75	514097.12	60242.815	60242.81
C_f	0.00416	0.00507	0.00541	0.00541
C_{Dmin}	0.01043	0.01770	0.01348	0.01348
TOTAL C_{Dmin}			0.0551	

The inviscid or induced drag factor is given by Equation below

$$K' = \frac{1}{\pi ARe} \text{.....(12)}$$

AR represents the wing aspect ratio and e is the wingspan efficiency. K', AR and 'e' were calculated to be 0.041, 8.165 and 0.95 respectively.

C_{Lmin} was determined as the point of lowest C_D from the drag polar as shown in figure 1. Then, the viscous induced drag factor K'' is determined as the slope of the nearly linear relation as shown in figure 2.C_{Lmin} is computed as 1.1221 at a Reynolds number of 100,000 for the wing and K'' is found to equal to 0.1715.

Finally, these values can be substituted back into CD equation to obtain the airplane's 3D drag coefficient for all airfoil lift coefficients. Figure 3shows this relationship and the lift to

ISSN (O): 2393-8609

International Journal of Aerospace and Mechanical Engineering

Volume 4 – No.2, April 2017

drag ratio.Figure3 shows to a lift coefficient of about 0.7, drag coefficient of 0.076 at highest lift to drag ratio of 9.11.

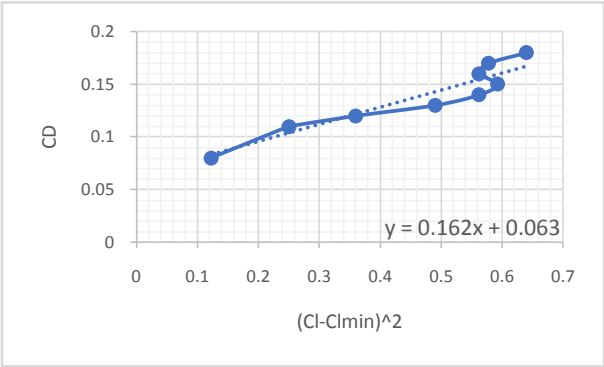

Fig 2: Graph of CD v/s (Cl-Clmin)^2

In addition, the equation shown is used to determine the total resulting 3D drag for the airplane traveling in one direction at 36 feet per second. The final Drag-Polar equation is given below:

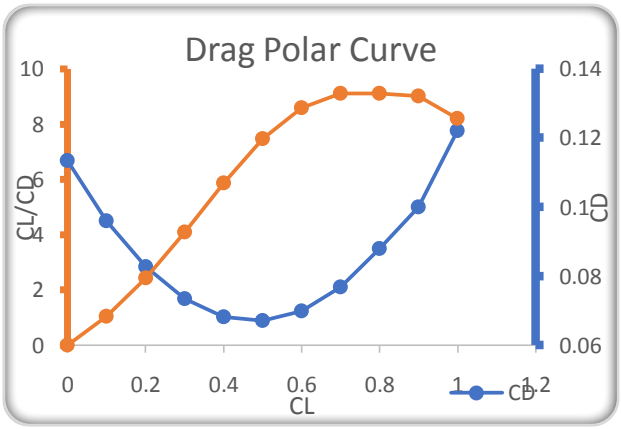

Fig 3: Graph of CL v/s Cl/CD and CL v/s CD

$$C_D = 0.055 + 0.041C_L^2 + 0.1621(C_L - 0.6)^2$$

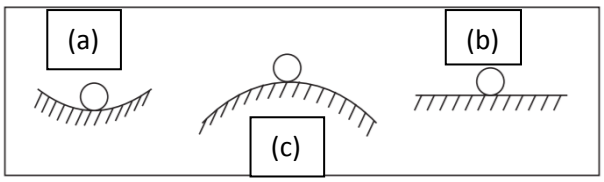

4. STABILITY AND CONTROL

1. Stability is the tendency of an airplane in flight to remain in straight, level, upright flight and to return to this attitude, if displaced, without corrective action by the pilot.

2. Static stability is the *initial* tendency of an airplane, when disturbed, to return to the original position. **Dynamic stability** is the *overall* tendency of an airplane to return to its original position, following a series of damped out oscillations.

Stability may be

(a) **positive,** meaning the airplane will develop forces or moments which tend to restore it to its original position;

(b) **neutral,** meaning the restoring forces are absent and the airplane will neither return from its disturbed position, nor move further away;

(c) **negative,** meaning it will develop forces or moments which tend to move it further away. Negative stability is, in other words, the condition of **instability.**

Static stability is determined by the aircraft's static margin, which is a measure of the relative positions of the aircraft center of gravity (CG) and neutral point (NP). The neutral point is a property of the configuration. If the CG is forward of the neutral point, small perturbations in pitch will create a restoring moment, eventually returning the plane to its original altitude, thus the configuration is stable. However, if the CG is too far forward, it can become very difficult to trim the aircraft and controllability can be reduced significantly.

The static margin is given by:

$$SM = \left(\frac{X_{CG} - X_{NP}}{MAC}\right) * 100\% \text{.....(13)}$$

Most aircraft tend to have static margins between 5% and 20%. Thus, this range was chosen as acceptable for the plane. The empty CG is located at 25% of the mean aerodynamic chord (MAC), the loaded CG is at 30% MAC, and the neutral point is at 37% MAC. Thus, the static margin in the empty and loaded cases are 7% and 12%, respectively. Though on the low side, these values are sufficient for static stability. They are also small enough that controllability should not be an issue.

FOM for different configurations of the tail is studied which clearly shows that the conventional configuration is the best among all. So the conventional configuration is the one which gives stability and is easy to manufacture and also fly.

4.1 Design of Horizontal Tail

The horizontal tail volume co-efficient is given by

$$V_h = \frac{l_h S_h}{S_w \bar{c}} \text{.....(14)}$$

V_h = Tail Co-efficient
S_w = Area of wing
S_v = Area of Horizontal tail
l_v = distance from c.g. to a.c. of vertical tail
b = Span

$V_h$from volume graph is found to be 0.5, and the wing area, chord being – 130045mm^2 and 130mm respectively, the optimum tail area is18232mm^2. The area that will be eliminated at the fixture is added by increasing the chord length and span. Finally, the dimensions of the horizontal tail to be:

Table 4. Dimensions of Horizontal tail

SPAN	250mm
WIDTH	80mm

ISSN (O): 2393-8609

International Journal of Aerospace and Mechanical Engineering

Volume 4 – No.2, April 2017

4.2 Design of Vertical Tail

The vertical tail volume co-efficient is given by

$$V_v = \frac{l_v S_v}{S_w b} \text{.....(15)}$$

V_h = Tail Co-efficient

S_w = Area of wing

S_h = Area of Horizontal tail

l_h = distance from c.g. to a.c. of horizontal tail

Vv from volume graph is found to be 0.03, and the wing area, wing span being – 130045mm2 and 130mm respectively, the optimum tail area is8084mm2. 100% of the area of total tail area is considered for the elevator and rudder. With regard to the above calculations an inverted flat plate is selected since it can satisfy all the moment balancing requirements arising from the pitch moment generated by the main wing and thus optimum stability was obtained. The stabilator and rudder will give the necessary stability as well as quick response to small deflections.

Table 5. Dimensions of Vertical tail

SPAN	120mm
WIDTH	80mm

5. FEM SPAR ANALYSIS USING ANSYS

Wings are the most essential part of an aircraft. Analyzing the forces which act on the wing will play an important role and is analogous to stability of the plane. In order to determine the forces that exist on the wings when attached to the fuselage, we threat this case as a simple cantilever beam that experiences a distributed load along its length. This load is the lifting force. The Stress and vertical displacement is given by the expressions

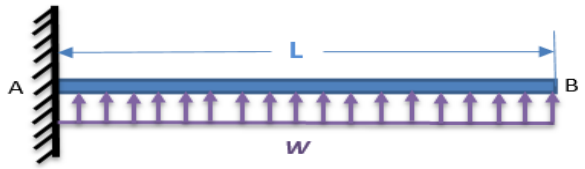

Fig 5: FEM Model of Wing spar

σmax = 0.5WL2c/I ……(16)

ymax = WL4/8EI……...(17)

'AB' is the wing, 'W' is the distributed load in lbs. per inch and 'L' is the half span of the wing, 'E' is the young's modulus for the spar's material, 'I' is the area moment of the spars cross-section, and c is the outer radius of the spar cross-section.

Static load tests were carried out by applying a distributed load along the lower portion of the main spar, with the innermost rib fixed in place to simulate the effect of fuselage integration. This spanwise load distribution is calculated and is assumed to be uniform along the length. Balsa Wood was considered isotropic material for the analysis. The normal load that the wing will experience during flight is 'g'. The critical load that the plane experiences is '2g' condition. The wing was analyzed in both the conditions using ANSYS Static Structural Workbench. The stress acting on the wing at the above loading conditions were analyzed and the deflection of the wing due to self-weight and during loading conditions was determined. A load of 2000g was uniformly distributed along the span of the wing for 'g' condition and 4000g for '2g' condition. The geometry was designed and an unstructured mesh was created to solve the problem.

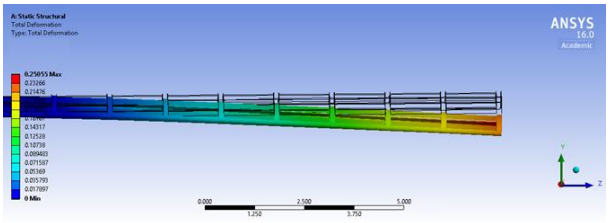

Fig 6: Deflection of the wing due to self-weight

The deformation due to self-weight and during loading conditions are as shown in the figure above and below respectively. The wing deflected by 0.25mm at the end during unloaded condition and 0.18mm during loading condition. There is 0.0260 of anhedral in the self-weight condition which is corrected by 0.0440 of dihedral angle with UDL condition with respect to the initial anhedral configuration

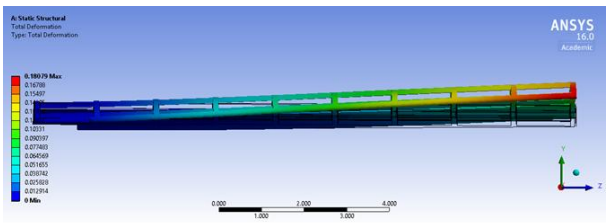

Fig 7: Upward deflection due to lifting force

The endurance analysis is done at '2g' condition where the wing was subjected to 4000g of load along the bottom spar which was deflected by 0.57mm . The analysis concluded that the wing will not break and is in the safe limits. The Von-Mises stress experienced by the wing during loading was checked which was within the elastic limits of balsa wood which has tensile ultimate strength of 18MPa with FOS 2.14.

6. MANUFACTURING

The need to further refine and push the envelope of the manufacturing techniques developed in the past and create a high lifting plane. Different processes were considered and qualitatively compared to the built-up balsa technique.

Literature survey on different materials found out that the birch wood pad was perfect for mounting the motor to the fuselage and the other sections made of the balsa expect the pad which carries the stabilator and the vertical tail.

6.1 Wing

Wing was totally made of balsa wood which made it strong and at the same time with minimum weight. To reduce weight sections of different planforms were cut according to the design easement and a thin spar with square section at the maximum pressure vector is used to reduce weight.The whole wing is then wraped with Ultrakote which is much lighter than monokote and also sticks to the surface with less waviness. The whole wing has a planform of 1098mm and chord length of 131mm with tapered ailerons with taper ratio 0.25 with length 480mm and the larger width of aileron is 30mm.

ISSN (O): 2393-8609

International Journal of Aerospace and Mechanical Engineering

Volume 4 – No.2, April 2017

6.2 Fuselage

For the fabrication easement, fuselage has rectangular sections which are sectioned from laser cutting which gives pin point accuracy. The placement of all the electronics inside fuselage was decided before designing. Separate area was allocated for battery placement, payload bay, ESC and receiver. The positions of all these components was in the front and they were placed considering the CG of the plane before and after the payloads are secured. The fuselage has a total length of 689mm and maximum width of 61mm. The motor mount is made up of birch wood which will withstand the forces generated by the motor because of its high structural strength compared with balsa wood. The idea was to secure the wing with the plate and bolting it to the fuselage, also 1/4th of the leading edge would be placed inside the fuselage to get secured fit.

6.3 Tail

The conventional inverted-T tail design was chosen and the balsa wood is laser cut according to design. The pad of stabilator and the vertical tail is made of balsa which can sustain lift generated by the stabilator for pitching and also the movement of the vertical tail. For good response of the tail the team decided to use the stabilator. To increase the performance of the tail NACA 0012 airfoil is used to manufacture tail instead of using the conventional 5 mm thick balsa sheet of same area. The stabilator has the dimension 250 X 80mm and the rudder has the dimensions 120 X 80 mm. The tail and Prototype plane image is as shown below.

Fig 8: Final Construction of the Plane in propel lab-3

7. REFERENCES

[1] UIUC Applied Aerodynamics Group, UIUC Airfoil Coordinates Database.

[2] www.ae.illinois.edu/m-selig/ads/coord_database.html

[3] Carpenter and Houghton, “Aerodynamics for Engineering students”, Butterworth and Heinemann, 17March 2003.

[4] Raymer, Daniel P. 1999 “Aircraft design, A conceptual approach” AIAA Alexander Bell Drive and Reston. October 15, 2009.

[5] WB Garner, Model Airplane Propellers. March 2009

[6] http://www.dcrc.org/pdf/Model%20Propellers%20Article.pdf

[7] Selig, Michael S. “High-Lift Low Reynolds Number Airfoil Design”. Published in Journal of Aircraft, Vol. 34, No. 1, January-February 1997

[8] Wilcox, David C (1998). "Turbulence Modeling for CFD". Second edition. Anaheim: DCW Industries, 1998. pp. 174.